

An Inverse Finite Element Method for Reconstruction of Elastic Deformations in Beam, Plate and Shell Structures

Alex Tessler

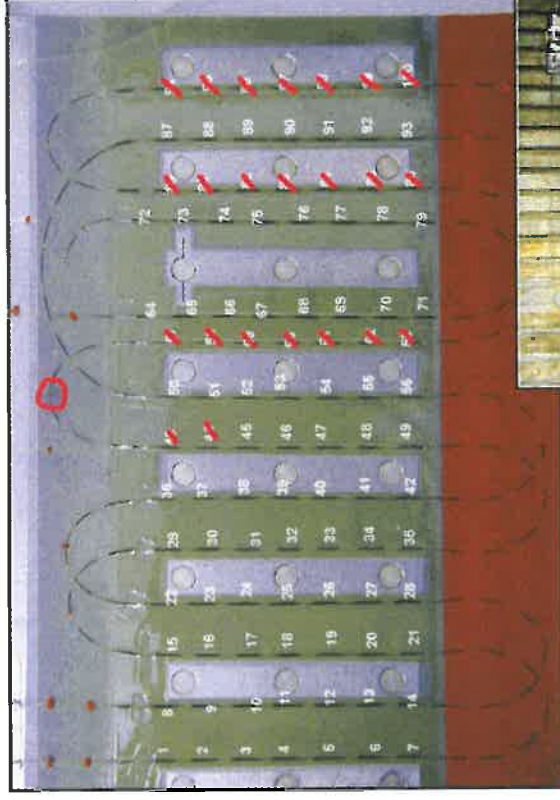
Analytical and Computational Methods Branch
NASA Langley Research Center, Virginia, U.S.A.

Jan L. Spangler

Lockheed Martin Aeronautics Company
NASA Langley Research Center, Virginia, U.S.A.

Structural health monitoring

- Civil and aeronautical structures
- Fiber optic Bragg-grating sensors measure
 - Strains
 - Temperatures
- Full-field quantities of interest (in real time)
 - Displacements (morphing wing, radar antenna)
 - Strains
 - Stresses
 - Failure criteria



Objective

- Develop fast and robust algorithm for reconstruction of full-field displacements from measured strains – an inverse problem

Approach

- Minimize Error Functional (variational principle)
- Inverse Boundary Value Problem
- Inverse FEM (Strain Integration Algorithm)



Strain
Integration
Algorithm



Outline

- Inverse reconstruction problem
- First-order shear deformation theory
- Penalty error functional
- Inverse finite element method
- Computational validation
- Computational-experimental validation
- Summary

Inverse reconstruction problem

- Inverse problems are ill-posed
 - Do not satisfy conditions of existence, uniqueness, and stability
- Uniqueness
 - various strains and boundary conditions that correspond to nearly same displacements
- Instability
 - Small disturbances in measured data (strains) cause great changes in solution (displacements)
- Tikhonov's regularization method
 - Improves robustness of algorithms by enforcing additional physical constraints ensuring smoothness of solution

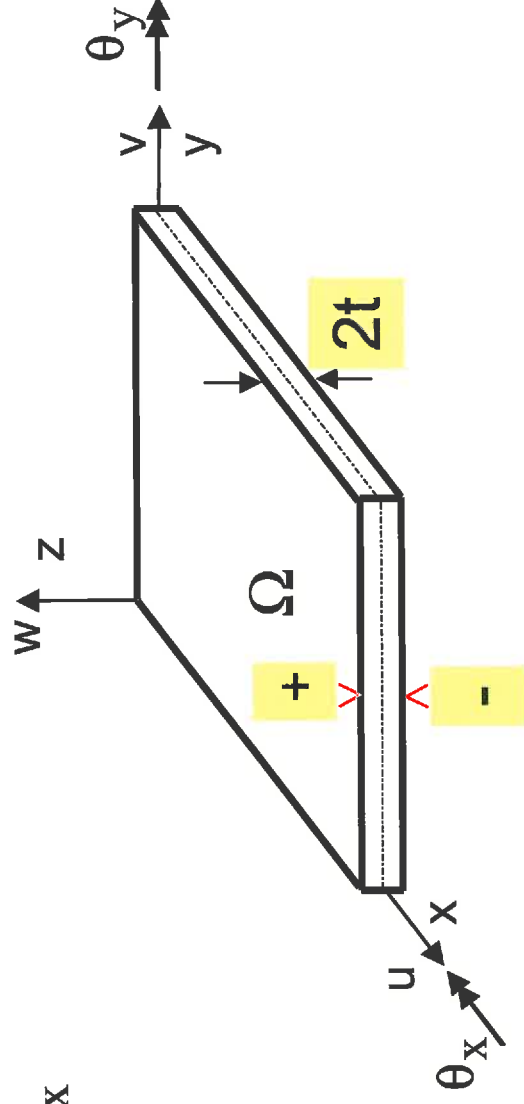
First-order shear deformation theory

- Displacements

$$u_x(x, y, z) = u + z\theta_y$$

$$u_y(x, y, z) = v + z\theta_x$$

$$u_z(x, y, z) = w$$



Strain-displacement relations

- In-plane strains

$$\boldsymbol{\varepsilon} \equiv \begin{bmatrix} \frac{\partial}{\partial x} & 0 & \frac{\partial}{\partial y} \\ 0 & 0 & 0 \\ 0 & \frac{\partial}{\partial y} & \frac{\partial}{\partial x} \\ 0 & 0 & 0 \\ 0 & 0 & 0 \\ 0 & 0 & 0 \end{bmatrix} \begin{Bmatrix} u \\ v \\ w \\ \theta_x \\ \theta_y \end{Bmatrix}$$

$$\begin{Bmatrix} \varepsilon_{xx} \\ \varepsilon_{yy} \\ \gamma_{xy} \end{Bmatrix} = \begin{Bmatrix} \varepsilon_{x0} \\ \varepsilon_{y0} \\ \gamma_{xy0} \end{Bmatrix} + \mathbf{z} \begin{Bmatrix} \kappa_{x0} \\ \kappa_{y0} \\ \kappa_{xy0} \end{Bmatrix}$$

$$\mathbf{K} \equiv \begin{bmatrix} 0 & 0 & 0 & \frac{\partial}{\partial x} & 0 \\ 0 & 0 & 0 & 0 & \frac{\partial}{\partial y} \\ 0 & 0 & 0 & \frac{\partial}{\partial y} & \frac{\partial}{\partial x} \\ 0 & 0 & 0 & 0 & 0 \\ 0 & 0 & 0 & 0 & 0 \end{bmatrix} \begin{Bmatrix} u \\ v \\ w \\ \theta_x \\ \theta_y \end{Bmatrix}$$

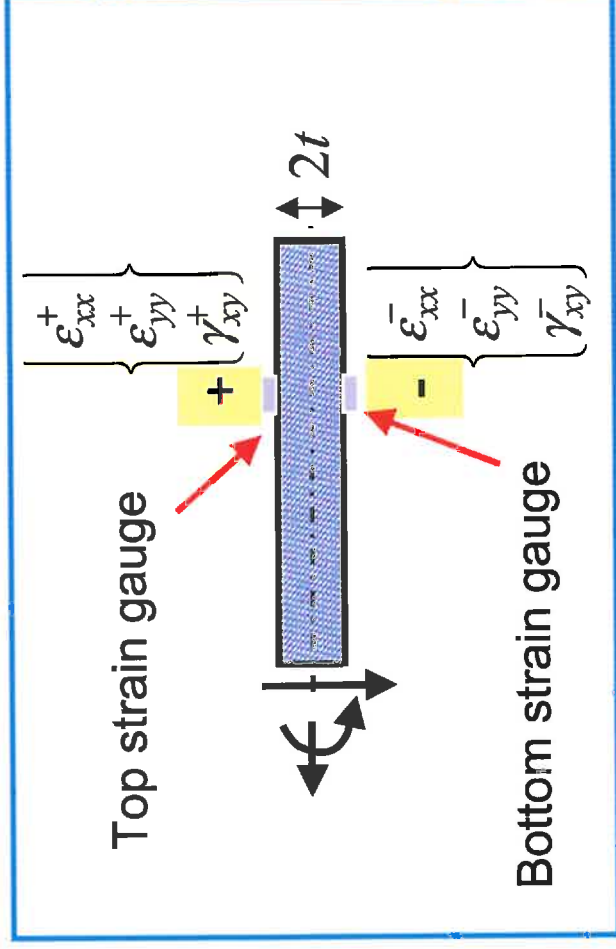
- Transverse shear strains

$$\boldsymbol{\gamma} \equiv \begin{Bmatrix} \gamma_{xzo} \\ \gamma_{yzo} \end{Bmatrix} = \begin{bmatrix} 0 & 0 & \frac{\partial}{\partial x} & 0 & 1 \\ 0 & 0 & \frac{\partial}{\partial y} & 1 & 0 \end{bmatrix} \begin{Bmatrix} u \\ v \\ w \\ \theta_x \\ \theta_y \end{Bmatrix}$$

Measured strains

$$\begin{Bmatrix} \varepsilon_{x0} \\ \varepsilon_{y0} \\ \gamma_{xy0} \end{Bmatrix}^{\delta} = \frac{1}{2} \left(\begin{Bmatrix} \varepsilon_{xx}^+ \\ \varepsilon_{yy}^+ \\ \gamma_{xy}^+ \end{Bmatrix} + \begin{Bmatrix} \varepsilon_{xx}^- \\ \varepsilon_{yy}^- \\ \gamma_{xy}^- \end{Bmatrix} \right)$$

$$\begin{Bmatrix} K_{x0} \\ K_{y0} \\ K_{xy0} \end{Bmatrix}^{\delta} = \frac{1}{2t} \left(\begin{Bmatrix} \varepsilon_{xx}^+ \\ \varepsilon_{yy}^+ \\ \gamma_{xy}^+ \end{Bmatrix} - \begin{Bmatrix} \varepsilon_{xx}^- \\ \varepsilon_{yy}^- \\ \gamma_{xy}^- \end{Bmatrix} \right)$$



$$\begin{Bmatrix} \gamma_{xzo} \\ \gamma_{yzo} \end{Bmatrix}^{\delta} \quad \text{special method}$$

In thin plates
“measured” shear
strains can be omitted

Error smoothing functional

- Find an extremum of the smoothing functional for a fixed value of penalty parameter λ

$$\Phi^\lambda(\mathbf{u}^h) = \|\boldsymbol{\varepsilon}(\mathbf{u}^h) - \boldsymbol{\varepsilon}^\delta\|^2 + \|\boldsymbol{\kappa}(\mathbf{u}^h) - \boldsymbol{\kappa}^\delta\|^2 + \lambda \|\boldsymbol{\gamma}(\mathbf{u}^h) - \boldsymbol{\gamma}^\delta\|^2$$

Euclidean squared norms

$$\|\boldsymbol{\varepsilon}(\mathbf{u}^h) - \boldsymbol{\varepsilon}^\delta\|^2 \equiv \frac{1}{n} \sum_{i=1}^n [\boldsymbol{\varepsilon}(\mathbf{u}^h)_{\mathbf{x}_i} - \boldsymbol{\varepsilon}_i^\delta]^2$$

$$\|\boldsymbol{\kappa}(\mathbf{u}^h) - \boldsymbol{\kappa}^\delta\|^2 \equiv \frac{\Omega^e}{n} \sum_{i=1}^n [\boldsymbol{\kappa}(\mathbf{u}^h)_{\mathbf{x}_i} - \boldsymbol{\kappa}_i^\delta]^2$$

$$\|\boldsymbol{\gamma}(\mathbf{u}^h) - \boldsymbol{\gamma}^\delta\|^2 \equiv \frac{1}{n} \sum_{i=1}^n [\boldsymbol{\gamma}(\mathbf{u}^h)_{\mathbf{x}_i} - \boldsymbol{\gamma}_i^\delta]^2$$

- Weights in error functional $\{1, 1, \lambda\}$

- 2nd and 3rd terms coupled

- Generally $\lambda \ll 1$

$\boldsymbol{\varepsilon}_i^\delta, \boldsymbol{\kappa}_i^\delta, \boldsymbol{\gamma}_i^\delta$ Arrays of measured strains at \mathbf{x}_i

Special case: Thin plates and shells

- 3rd term

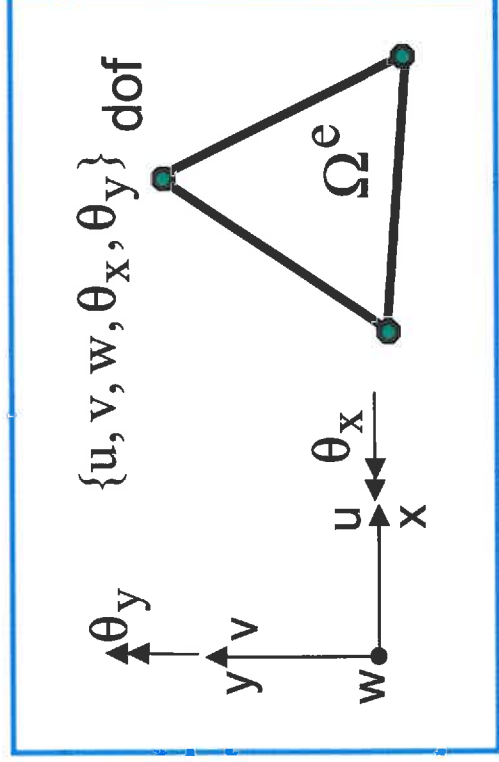
$$\lambda \|\gamma(\mathbf{u}^h) - \gamma\|^2 \equiv \frac{\lambda}{\Omega^e} \int_{\Omega^e} \gamma(\mathbf{u}^h)^2 dx dy$$

- Kirchhoff constraints enforced

$$\left\{ \begin{array}{l} \gamma_{xzo} \\ \gamma_{yzo} \end{array} \right\} \equiv \left\{ \begin{array}{l} w_{,x} + \theta_y \\ w_{,y} + \theta_x \end{array} \right\} \rightarrow 0$$

Kinematic interpolations for inverse flat shell element (MIN3⁻¹)

$$\mathbf{u}^h \equiv \begin{Bmatrix} u \\ v \\ w \\ \theta_x \\ \theta_y \end{Bmatrix} \equiv \mathbf{N} \mathbf{d} \begin{Bmatrix} \text{linear} \\ \text{linear} \\ \text{quadratic} \\ \text{linear} \\ \text{linear} \end{Bmatrix}$$



$\mathbf{u}^h \equiv \mathbf{N} \mathbf{d}$ *anisoparametric*

N: C^0 – continuous shape functions

d: displacement dof's

Tessler-Hughes, CMAME (1985)

$$\begin{Bmatrix} \epsilon_{x0} \\ \epsilon_{y0} \\ \gamma_{xy0} \end{Bmatrix} \text{ constant} \quad \begin{Bmatrix} K_{x0} \\ K_{y0} \\ K_{xy0} \end{Bmatrix} \text{ constant} \quad \begin{Bmatrix} \gamma_{xz0} \\ \gamma_{yz0} \end{Bmatrix} \text{ linear}$$



Inverse FEM equations

- Minimize sum of element contributions

$$\delta \left[\sum_{e=1}^N \Phi_e^\lambda(\mathbf{u}^h) \right] = 0$$

results in

$$\mathbf{d} = \mathbf{K}^{-1} \mathbf{F}$$

fast computation

$$\mathbf{K} \equiv \mathbf{K}(\mathbf{x}_i)$$

$$\mathbf{d} \equiv \mathbf{d}(\mathbf{u})$$

$$\mathbf{F} \equiv \mathbf{F}(\boldsymbol{\varepsilon}^0)$$

Symmetric, positive definite

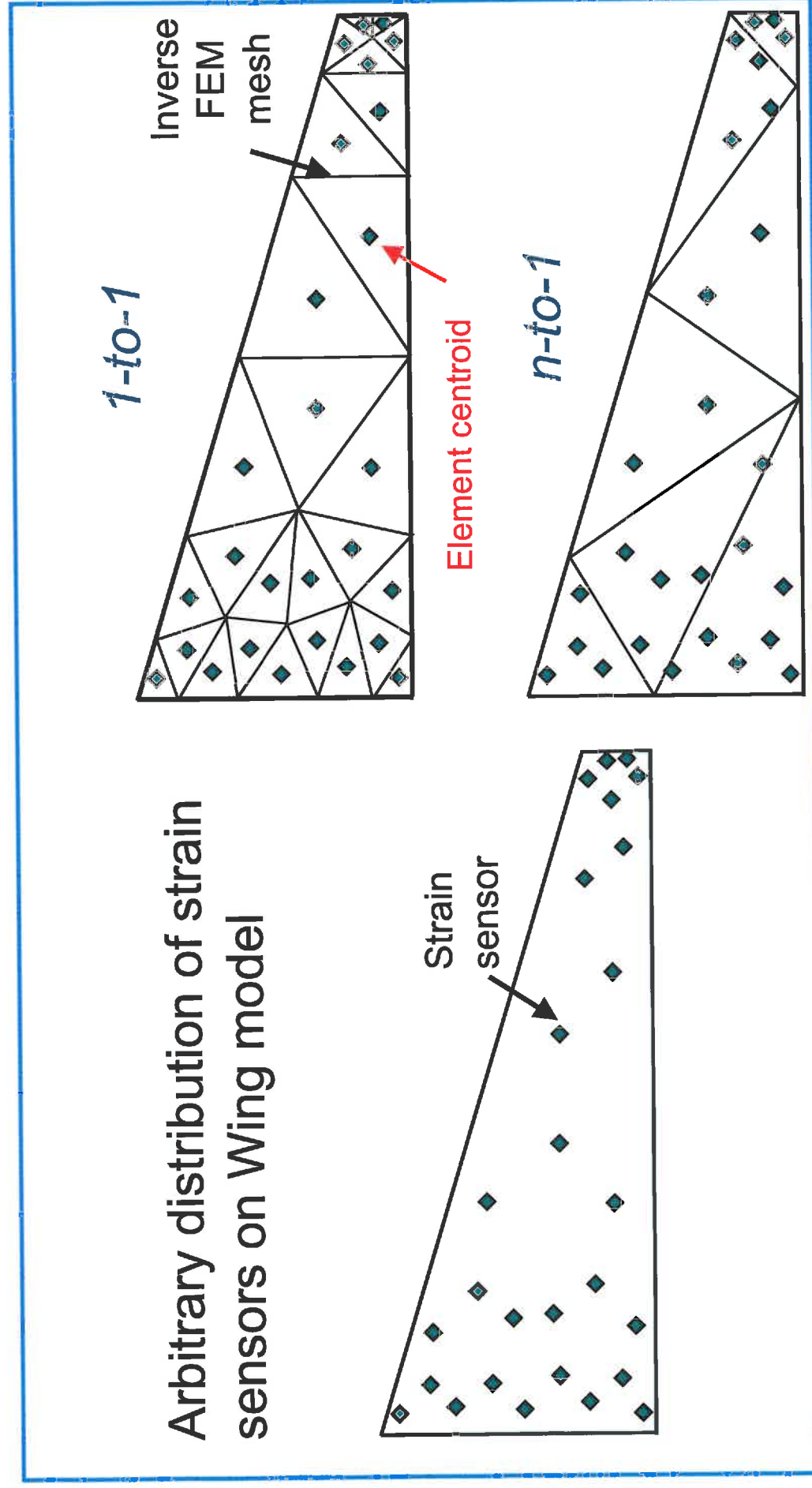
Displacement dof's

r.h.s. vector

Computational validation

- Direct FEM solution
 - Mesh, materials, loads and B.C.'s
 - Output strains at optimal points
- Inverse FEM solution
 - Direct analysis strains used as “experimental” strains
 - “Experimental” strains mapped onto inverse FEM mesh
 - Apply same kinematic B.C.'s as in direct analysis
 - Solve inverse FEM equations to obtain displacements
- Comparison
 - reconstructed displacements vs. displacements from direct analysis

Inverse FEM: Mapping of strains

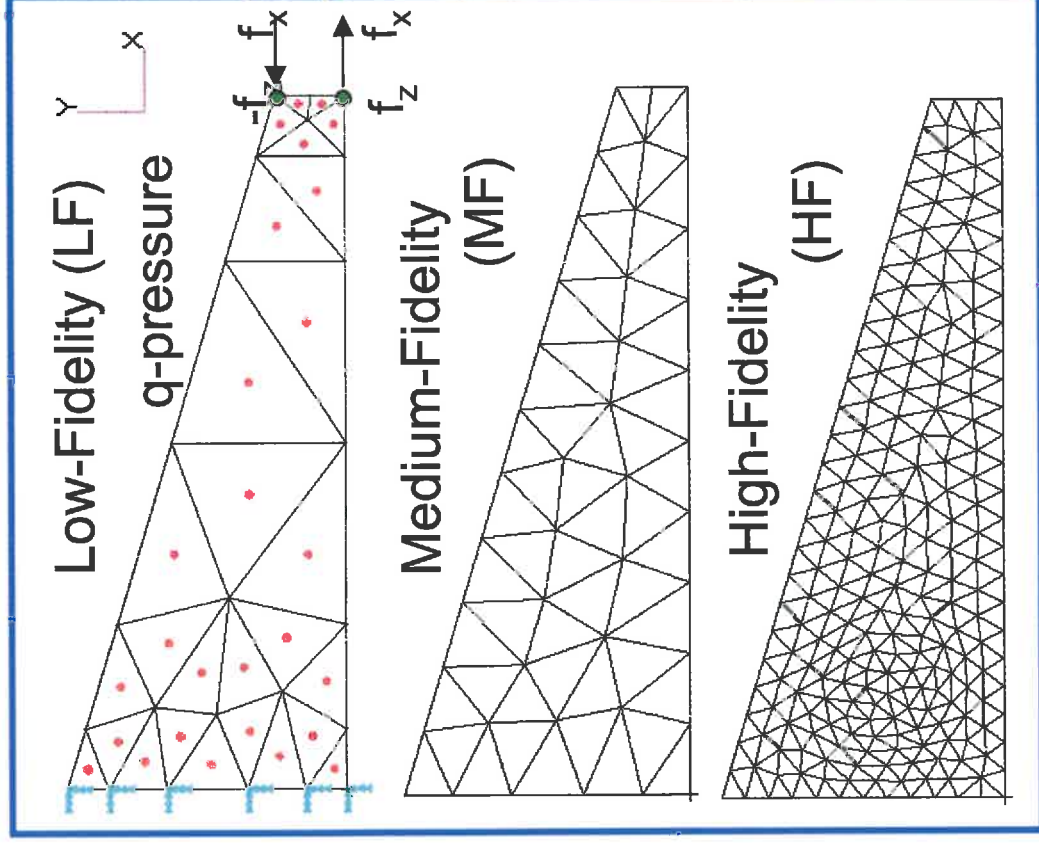


Idealized wing: Direct FE analysis

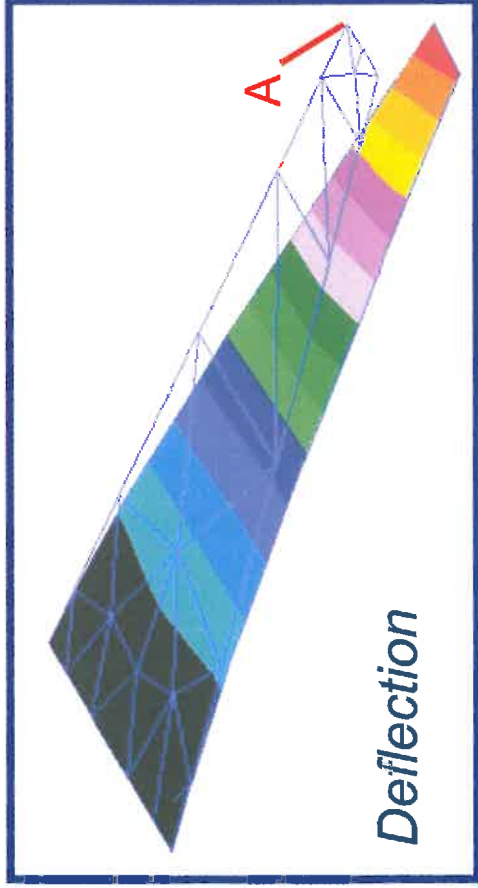
- Clamped AL panel
- Loads
 - Uniform pressure
 - Twisting forces
 - In-plane forces
- Span / thickness = $6 \cdot 10^4$

Direct FEM

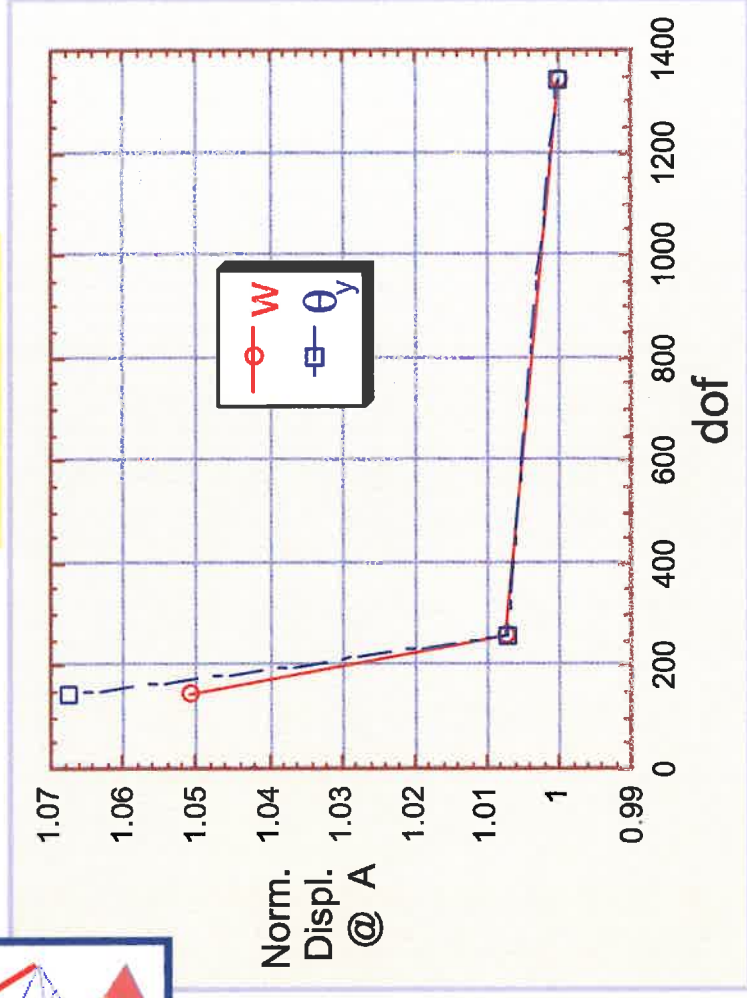
Element	Interpolations
MIN3	\mathbf{u}^h



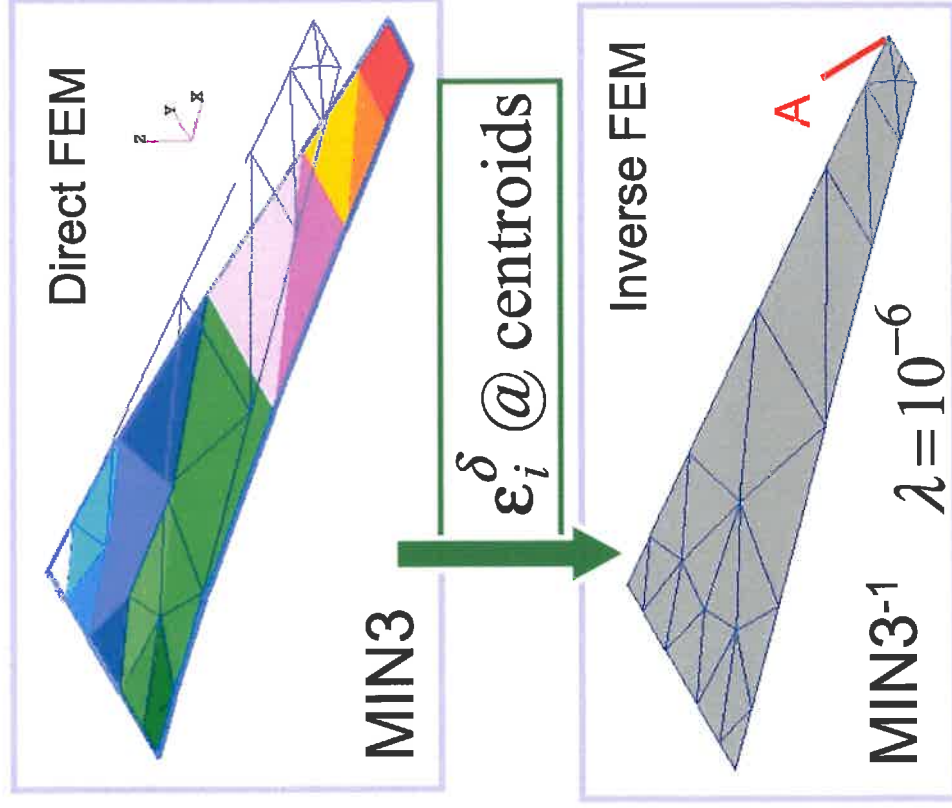
Direct FE analysis



Convergence of (w, θ_y) point A



Inverse FEM using 1-1 mapping of strains from MIN3 analysis

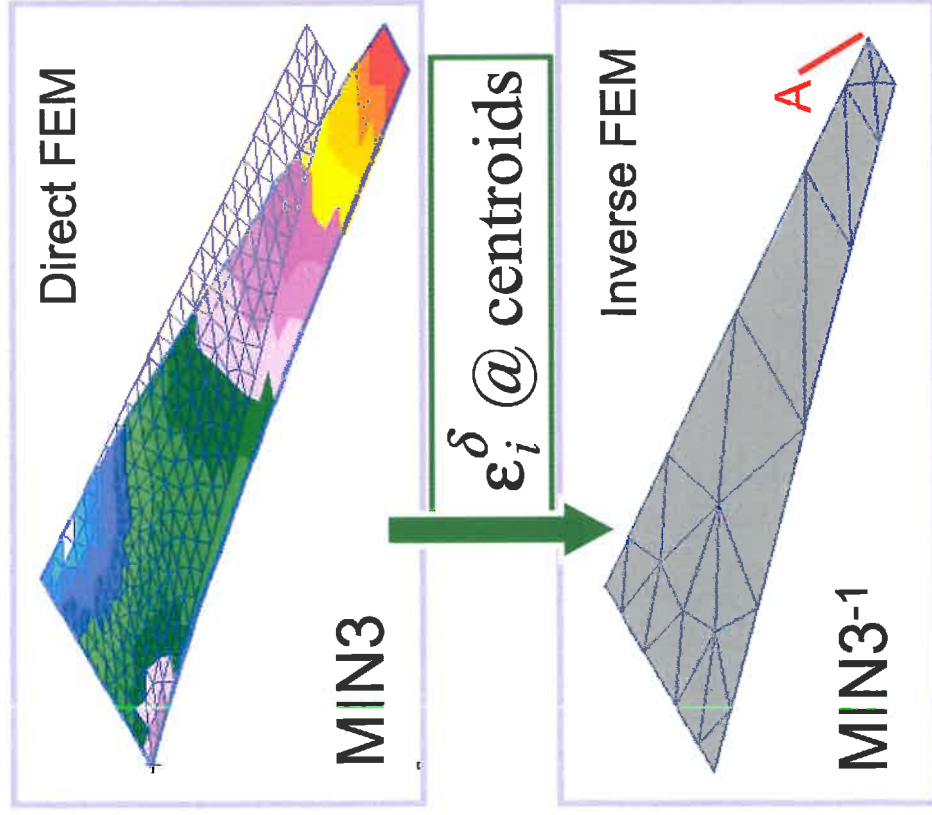


- Exact reconstruction of

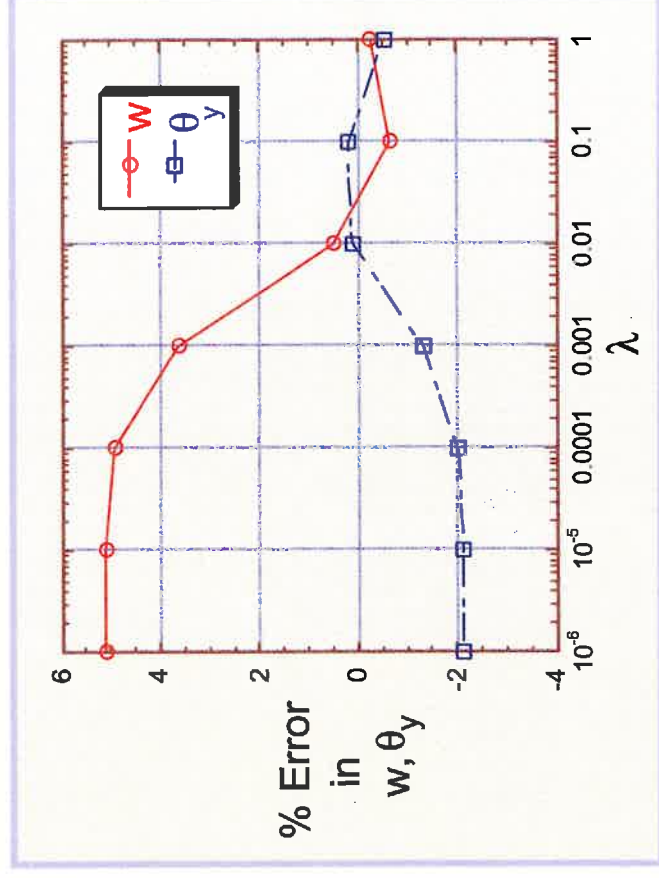
$$(u, v, w, \theta_x, \theta_y)$$

for all meshes

Inverse FEM using n-1 mapping of strains from MIN3 analysis



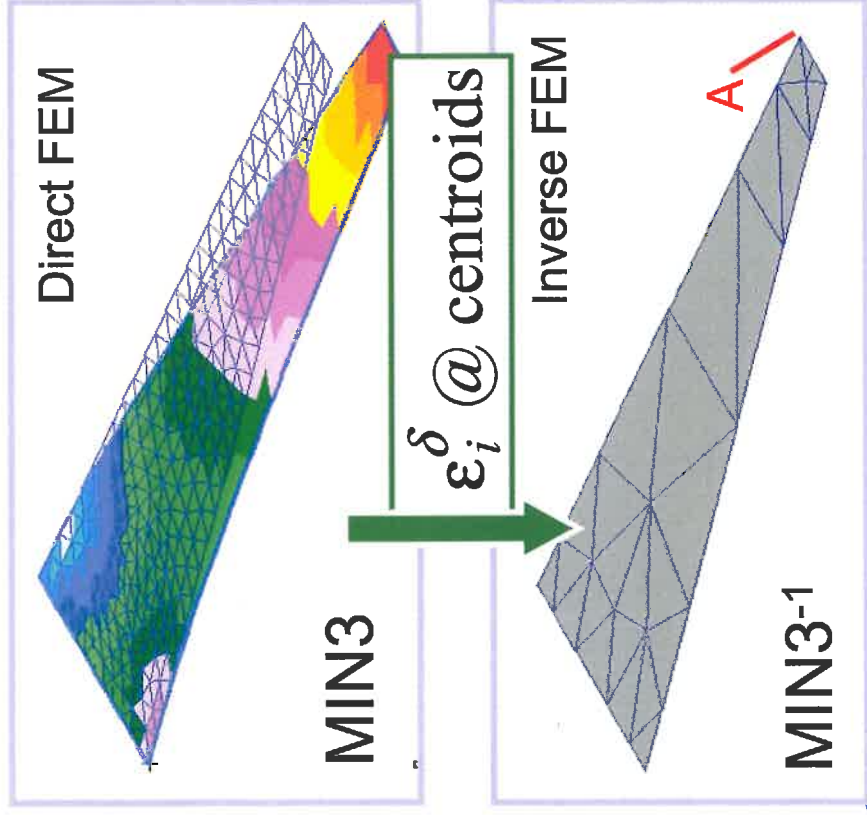
Lambda study



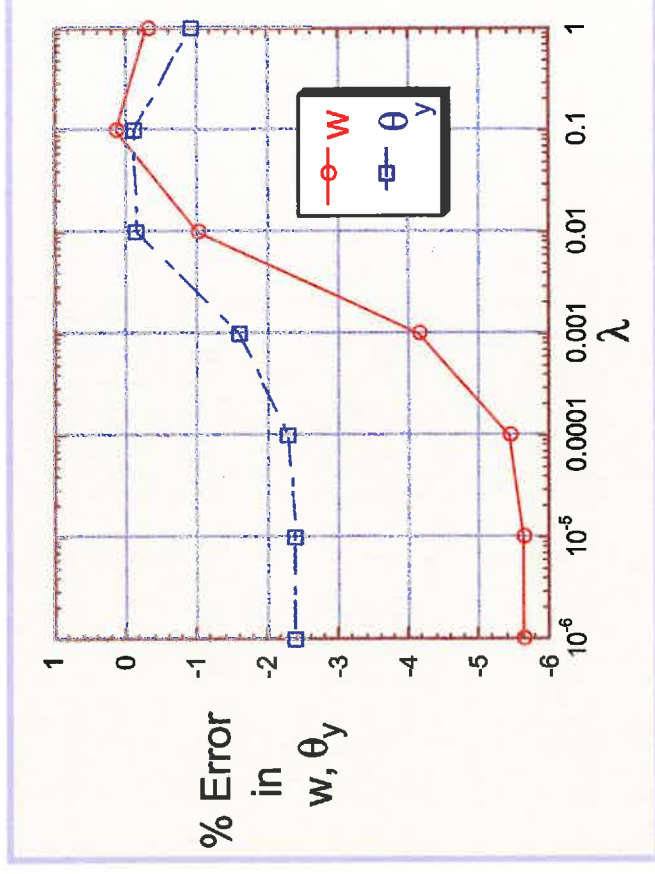
Strains with Random Error

$$\epsilon^\delta = \epsilon * (1 + 0.05 * \delta),$$

$\delta \in [-1, 1]$ (pseudorandom number)



Lambda study

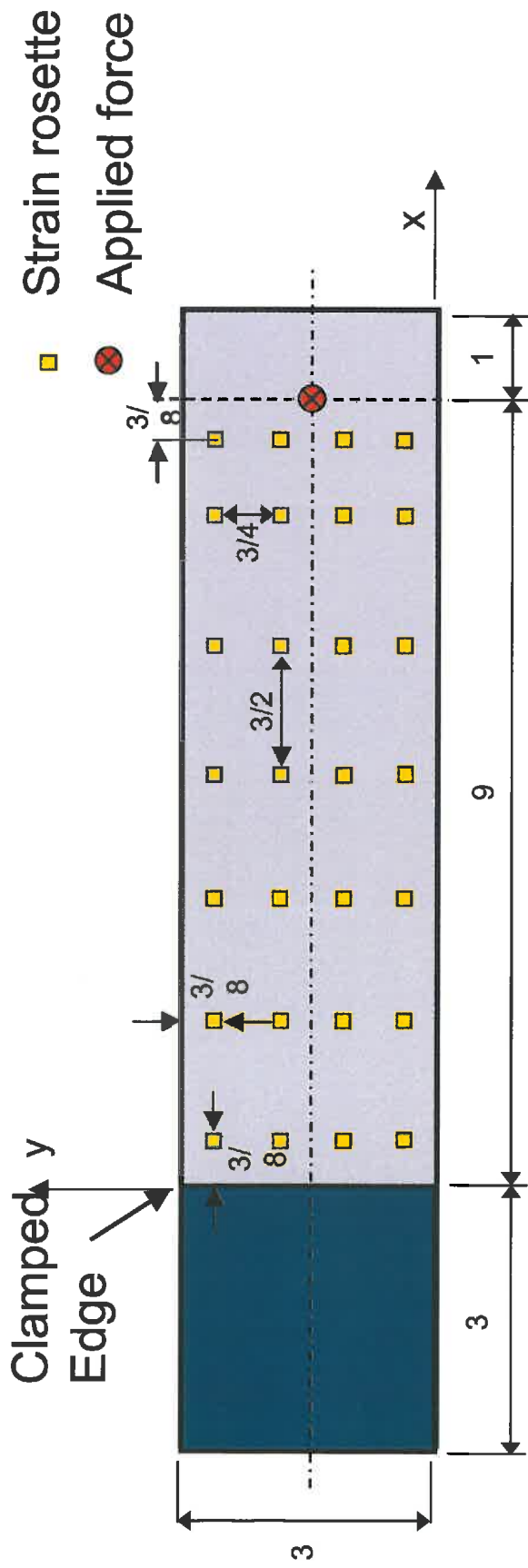
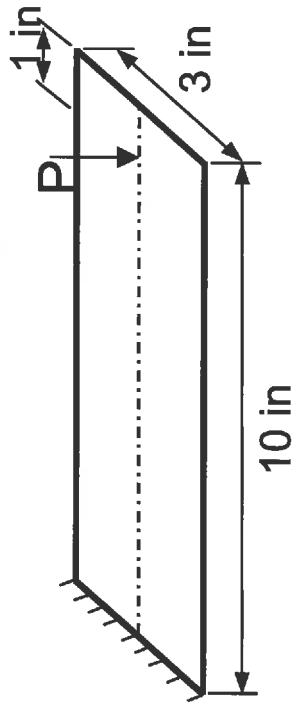


Remarks on Numerical Results

- **MIN3⁻¹ exact inverse of MIN3**
 - Perfect correspondence in 1-1 mapping
 - Strains sampled at element centroids
- **No thin-regime limitations**
- **Lambda parameter ensures robustness**
 - Serves as filter/smoother for n-1 mapping
 - Strains with random error “smoothed” effectively

Computational-experimental validation

- Aluminum plate, 2024-T3 alloy
 - Elastic properties: $E=10.6$ Msi, $\nu=0.33$
 - Dimensions: $10'' \times 3'' \times 1/8''$
- Force applied at (9", 1.5")
 - $P = 5.784$ lb (2623 g)



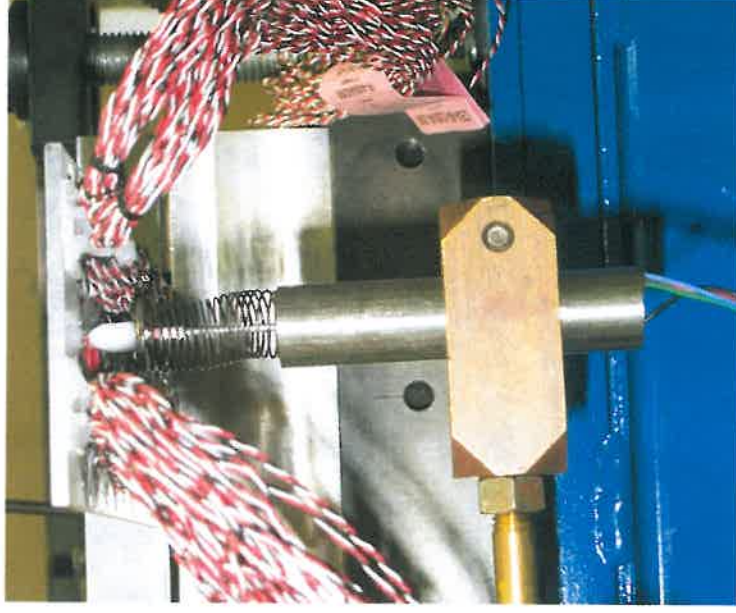
All dimensions in inches

Experiment

Plate instrumented with
28 strain rosettes and DCDT

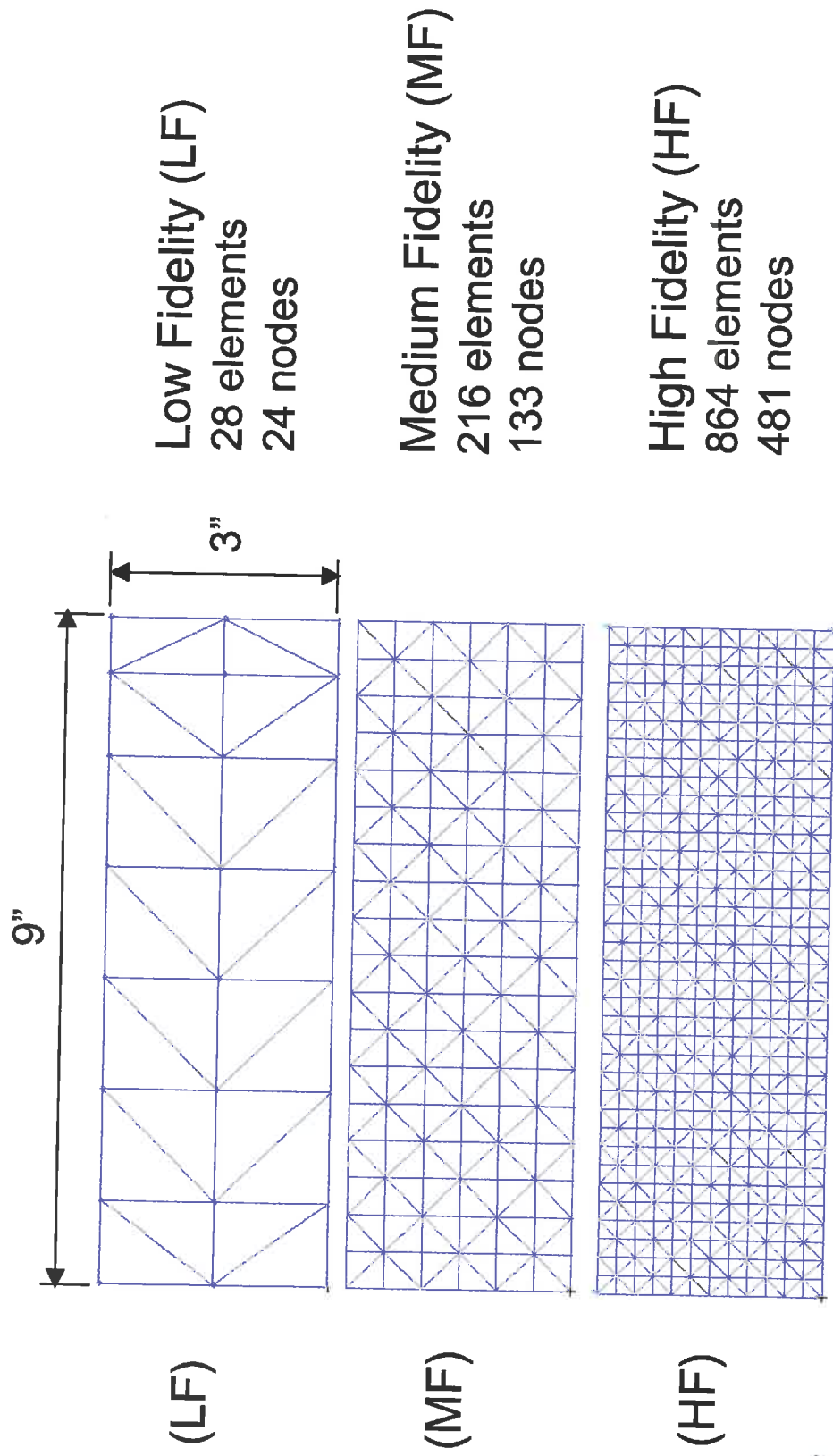


DCDT measuring deflection
@ (8 7/16, 1 1/2)



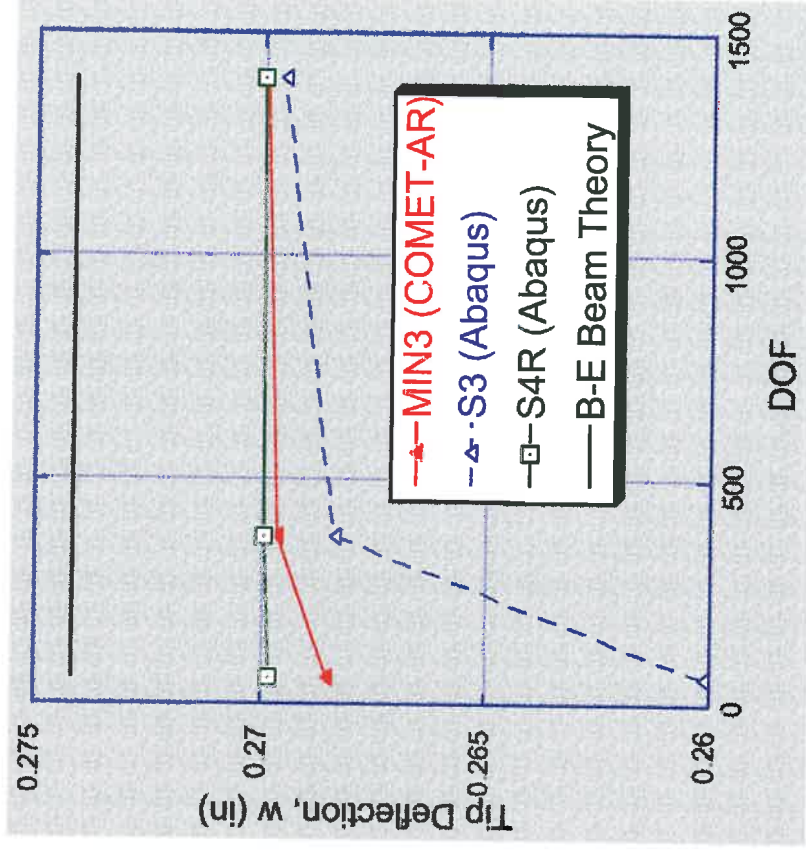
FE Modeling of Experiment

Triangular Element Meshes

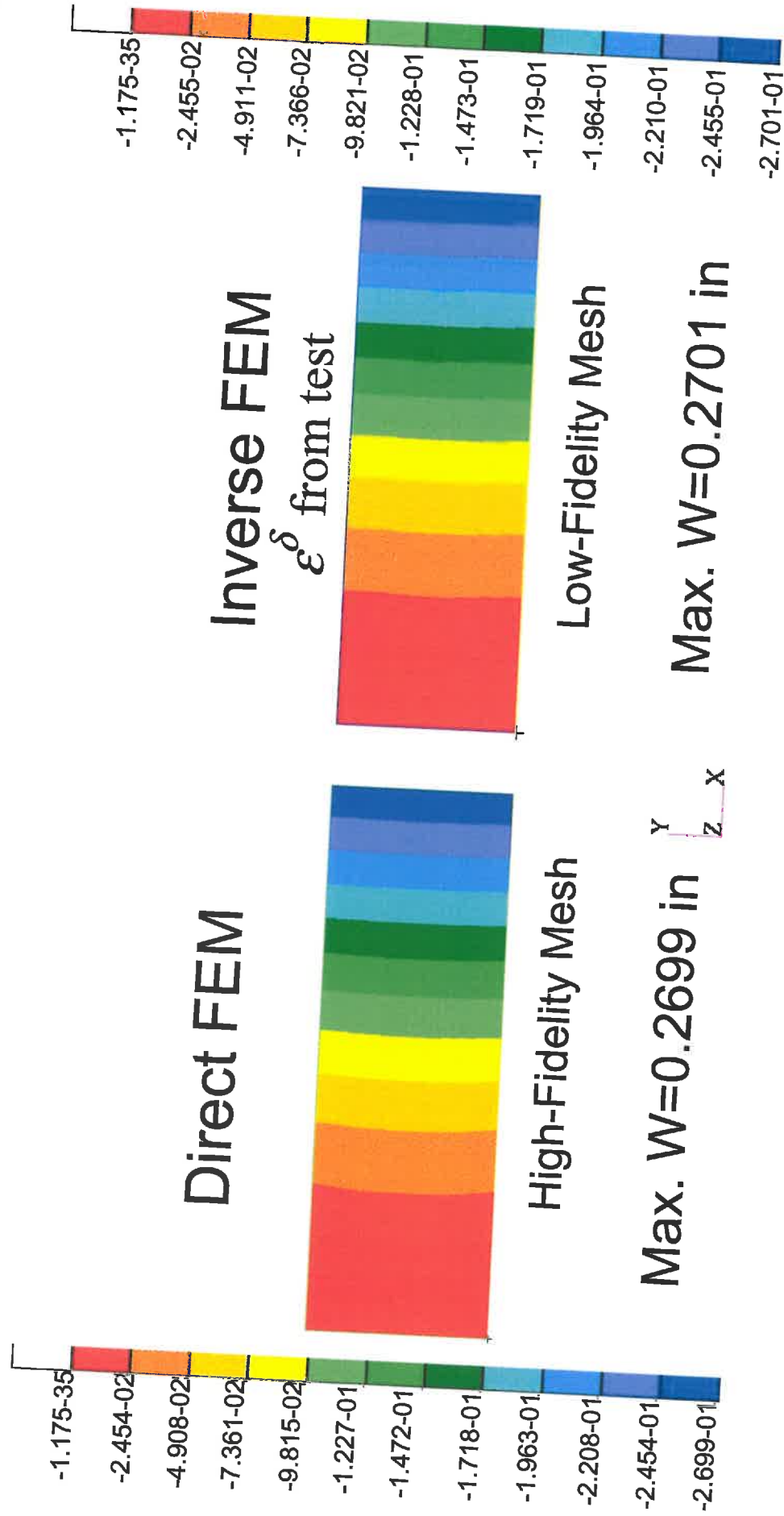


FEM convergence study of tip deflection

- Linear response
 - differences between linear and nonlinear solutions less than 0.01%



Comparison of Deflection



Summary

Variational principle and robust inverse FEM developed for full-field displacement reconstruction from measured strains

- Thin and moderately thick
 - Beams, plates and flat shells
 - Linear response
- Method inherently regularized
 - Strain-displacement relations enforced
 - Integrability (strain compatibility) conditions fulfilled
 - Strain-sensor location and mesh/interpolation dependency
- Standard FEM architecture
 - Accommodates complex structures
 - Independent of material properties
 - Computationally efficient

Summary (cont.)

- Superior reconstruction quality
 - Computational validation
 - Computational-Experimental validation
- Future extension to
 - Large displacement response
 - Non-collocated strain measurements
 - Full-field reconstruction of strains, stresses, and failure criteria
 - Curved shells
 - Built-up structures